

Multi-Start n -Dimensional Lattice Planning with Optimal Motion Primitives

Alexander Botros and Stephen L. Smith

Abstract—In the field of motion planning the use of pre-computed, feasible, locally optimal motions called motion primitives can not only increase the quality of motions, but decrease the computation time required to develop these motions. In this work we extend the results of our earlier work by developing a technique for computing primitives for a lattice that admits higher-order states like curvature, velocity, and acceleration. The technique involves computing a minimal set of motion primitives that t -span a configuration space lattice. A set of motion primitives t -span a lattice if, given a real number t greater or equal to one, any configuration in the lattice can be reached via a sequence of motion primitives whose cost is no more than t times the cost of the optimal path to that configuration. While motion primitives computed in this way could be used with any graph search algorithm to develop a motion, this paper also proposes one such algorithm which works well in practice in both short complex maneuvers and longer maneuvers. Finally, this paper proposes a shortcut-based smoothing algorithm based on shortest path planning in directed acyclic graphs.

I. INTRODUCTION

In the field of autonomous vehicle motion planning, a common technique for computing a motion between start and goal configurations involves a rough planning phase followed by a smoothing phase. Broadly, motion planning algorithms using this technique follow one of two approaches which we dub smoothing *up* and smoothing *out*. Regardless of approach, the planned motion must be feasible with respect to the non-holonomic constraints of the vehicle, collision-free, quickly computed, and optimal with respect to a pre-defined cost.

For motion planning problems involving many states and complex non-holonomic constraints, two point boundary variable (TPBV) problems may be computationally restrictive to solve. Thus, planners using the smoothing up approach compute a rough motion by, for example, decreasing the number of states or simplifying the non-holonomic constraints. Smoothing algorithms are then employed to increase the traversability of the rough motion. We call this approach smoothing *up* as the complexity of the rough path is increased to meet the constraints of the original problem. On the other hand, the smoothing out approach is categorized by computing a rough path in the full complexity of the original problem. This motion can then be smoothed using a variation of the shortcut technique [1] which leverages the triangle inequality to replace compound motions with direct motions where feasible.

A major benefit typical of the smoothing up technique is the speed with which a rough motion can be computed. However, the burden of returning a motion feasible for the vehicle rests on the smoother. Typically, smoothing algorithms



Fig. 1: Example of motion planning using t -spanning $G3$ motion primitives with configurations $(x, y, \theta, \kappa, \sigma, \rho)$. Magenta: primitives used during planning, Red: final motion, Cyan: car footprint.

in this approach return motions that are homotopic to the rough motion [2], [3]. This is a drawback of this approach as it may be the case that a rough motion is computed that does not lie within the same homotopy class as the optimal motion. A toy example of this drawback is illustrated in Figure 2. Here a path is computed between start and goal configurations with positions in \mathbb{R}^2 , and heading in $[0, 2\pi]$. Way-points were computed using an any-angle planner, and a Bezier spline curve is fit to those waypoints in such a way so as to minimize a trade-off between lateral path error and maximum curvature. Because the rough motion is computed using only states (x, y) , it admits TPBV solutions with instantaneously changing heading. This coupled with the tightness of the obstacles around the waypoints, results in a smoothed motion with prohibitively high curvature.

In contrast to the smoothing up approach, rough motions computed using the smoothing out approach are feasible. Thus, the burden of feasibility is no longer placed on the smoothing process. However, the computation time of a rough motion has the potential to be prohibitive owing to the complexity of the TPBV problems involved. As the complexity of these problems increases, the use of probabilistic sampling-based motion planning – which requires solving many TPBV problems – becomes impractical. In contrast, deterministic sampling-based motion planning facilitates the use of pre-computed feasible motions called *motion primitives* which can be re-used during planning. The use of these primitives reduces the number of TPBV problems that must be solved online resulting in easily computed feasible motions. This paper focuses on one class of deterministic sampling: *lattice* planning.

The high-level idea behind lattice planning, is to discretize a vehicle’s configuration space into a countable set (or *lattice*) of regularly repeating configurations. Motions between lattice

This work is supported in part by the Natural Sciences and Engineering Research Council of Canada (NSERC)

The authors are with the Department of Electrical and Computer Engineering, University of Waterloo, 200 University Ave W, Waterloo ON, Canada, N2L 3G1 (alexander.botros@uwaterloo.ca, stephen.smith@uwaterloo.ca)

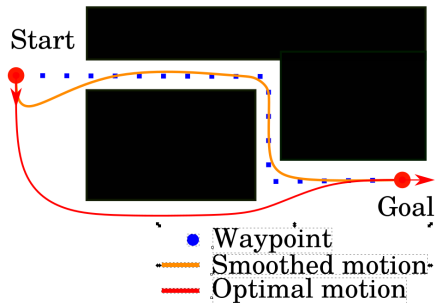


Fig. 2: Toy example: motion planning using the smoothing up approach with any-angle waypoints and Bezier smoothing.

configurations (or *vertices*) are pre-computed and a subset of these motions called a *control set* is selected [4], [5]. The motions should be feasible and possibly optimize some desirable property like arc-lengths, or comfort. Once the control set has been determined offline, the motions therein may be concatenated in real time to form more complex motions.

The regularity of the lattice structure allows for theoretical guarantees on the cost of lattice-optimal paths compared to free space optimal. The authors of [6] provide an upper bound on the ratio of costs of paths comprised entirely of concatenated lattice motions to those of optimal paths (under certain assumptions). These guarantees do not require the fineness of the lattice grid structure to approach infinity, which is typically not the case for probabilistic motion planning techniques like PRM, RRT, RRT*, etc.

In [7], we present a method for computing a control set of motion primitives based on the observation that the *number* of primitives in the control set favorably affects the quality of the resulting paths but adversely affects the performance of an online search. In [8] propose computing the the smallest control set that guarantees the existence of compound motions whose costs are no more than a factor of t from optimal. The authors of [8] also provide a heuristic for solving this problem, and in [7] we presented the first non-brute-force approach. This paper is an extension of our earlier work that addresses two critiques of lattice-based motion planning. The first is the zig-zag nature of resulting motions which can occur when pre-computed motions are concatenated. Secondly, in [7], we consider a single set of motion primitives. This does not allow for states like curvature, velocity, or non-cardinal heading. These extensions of our earlier work are outlined in the following section.

A. Contributions

The contributions of this work are fourfold:

- 1) We extend the definition of a lattice to include arbitrary vehicle states like velocity, curvature, etc.
- 2) We propose a method to compute a control set. This method involves computing a minimal t -spanning control set (MTSCS) for the extended lattice by way of a mixed integer linear program (MILP).
- 3) An A*-based algorithm to compute feasible motions (using the control set from contribution 2) for difficult maneuvers is presented.

- 4) We present a shortcut-based smoothing algorithm for motions computed using the algorithm from contribution 3. This algorithm runs in time quadratic in the number of vertices in the input motion and preserves the t -factor sub-optimality.

B. Related Work

Techniques using the smoothing up approach include fitting Bezier curves [9], or polynomial splines [10], [11] to a sequence of way-points. These way-points are commonly computed using any-angle path planners like Probabilistic Road Map (PRM) [12], Rapidly Exploring Random Trees (RRT) [13], or RRT* [14] that plan way-points in (x, y) only. In [15], the authors develop a path planner similar to the Fast Marching Tree (FMT) algorithm [16] that takes into account non-holonomic constraints. To keep computation time low, however, the authors assume affine dynamics which allows them to solve TPBV problems analytically. Rough paths developed with this simplified system are then smoothed in [3] in which motions with non-affine non-holonomic constraints and piece-wise linear velocity profiles are developed. This work illustrates the benefits of obtaining a rough path using a system of similar complexity to the desired final motion. However, by the very nature of the simplification, it is possible for infeasible rough paths to be developed. This is especially true when non-holonomic and obstacle constraints are used as terms in a cost function optimized by the smoother (as in [2]) instead of hard constraints.

The smoothing out approach is versatile in the problems it addresses. The authors of [17], [18] demonstrate lattice adaptations made to account for the structured environments of urban roads for use in autonomous driving, while in [19], a set of motion primitives is computed (based on experience) for a UAV exploring mine-shafts.

In the field of autonomous driving, the authors of [20] use six motion primitives for a Dubins' with forward and reverse motion. Motions are computed using a variant of the A* algorithm called Hybrid A*. Due to the discontinuity in curvature that appears in Dubins' paths, motions computed using such an approach have discontinuous curvatures. This results in motions with infinite instantaneous jerk, a known source of slip and discomfort for an autonomous vehicle [21]. On the other hand, the authors of [22] compute motion primitives that minimize the integral of the squared jerk over the motion but limit their results to forward motion.

The choice of motion primitives is of particular interest. Typically motion primitives are chosen to achieve certain objectives for the paths they generate. For example, in [23], the authors introduce the notion of probabilistic motion primitives which achieve a blending of deterministic motion primitives to better simulate real user behavior. The authors of [24] use Dispertio, a dispersion minimizing algorithm from [25] to compute a set of motion primitives that result in motions with minimum dispersion. In [4], on the other hand, the authors present the notion of using a minimal t -spanning set of motion primitives. That is, a set of motion primitives of the smallest size that guarantees that the cost of planned motions are within a factor of t from optimal. The notion of t -spanning motion primitives is similar to that of graph

t -spanners first proposed in [26]. Interestingly, dispersion-minimizing control sets and minimal t -spanning control sets both favor maximally *dissimilar* primitives allowing greater coverage of the configuration space. It should be noted that the primitives developed in this paper could be used in place of those computed in [19], [24] during motion planning.

In [8], the authors address the problem of computing a minimal set of t -spanning motion primitives for an arbitrary lattice. We refer to this problem as the minimum t -spanning control set (MTSCS) problem. For a Euclidean graph, attempting to determine such a minimum t -spanning set is known to be NP hard (see [27]), and in [8], the authors postulate that the same is true over an arbitrary lattice. The authors of [8] provide a heuristic for the MTSCS problem, which while computationally efficient, does not have any known guarantees on the size of the set relative to optimal.

In [7], we prove the NP-completeness of the MTSCS problem for a lattice with a single start, and reformulate the problem as a Mixed Integer Linear Program (MILP). As it will be further demonstrated here, a single start is often insufficient to capture the full complexity of a lattice. The work in [7] is expanded in [28], where the authors compute motions between lattice vertices that minimize a user-specified cost function that is learned from demonstrations. The work presented in this paper may be used in tandem with that in [7] to provide an improved set of motion primitives that mimic the driving style of a user.

II. MULTI-START LATTICE PLANNING

In this section, we introduce the notion of a multi-start lattice, and illustrate how they may be used in motion planning. We also formulate the Multi-start Minimum t -Spanning Control Set Problem that is the main focus of this work.

A. Multi-Start Lattices

Let \mathcal{X} denote the configuration space of a vehicle. That is, \mathcal{X} is a set of tuples – called *configurations* – whose entries are the *states* of the vehicle. Let $\mathcal{X}_{\text{obs}} \subset \mathcal{X}$ be a set of obstacles. A motion planning problem is:

Problem II.1 (Motion planning problem (MPP)). Given configuration space \mathcal{X} , obstacles \mathcal{X}_{obs} , start and goal configurations $p_s, p_g \in \mathcal{X} - \mathcal{X}_{\text{obs}}$, and a cost function c , compute a sequence of configurations – called a *motion* – from p_s to p_g such that

- 1) **Feasible motions:** Each configuration in the sequence is in $\mathcal{X} - \mathcal{X}_{\text{obs}}$, and the transition of each state in every configuration to the associated state in the next configuration in the sequence is dynamically feasible.
- 2) **Optimal motions:** The sequence minimizes c over all feasible sequences

Lattice-based planning approximates a solution to this problem by regularly discretizing \mathcal{X} using a *lattice*, $L \subseteq \mathcal{X}$. Typically, the error in cost incurred by such an approximation tends to zero as the as the lattice approaches \mathcal{X} .

Let i, j be vertices in L , and let p be a motion that solves Problem II.1 for $p_s = i, p_g = j$, written $i \cdot p = j$. The key behind lattice-based motion planning is the observation that p may be concatenated with other vertices in L potentially

resulting in another vertex in L . This observation motivates the use of a starting vertex $s \in L$, usually at the origin, that represents a prototypical lattice vertex. Offline, a feasible optimal motion is computed from s to all other vertices $i \in L$ in the absence of obstacles. Then a subset E of these motions is selected and used as an action set during online search. As such, the motions available at any iteration of the online search is isometric to those actions available at s . Unfortunately there

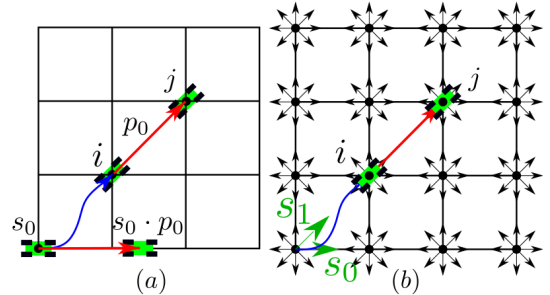


Fig. 3: (a) Lattice in $\mathcal{X} = \mathbb{R}^2 \times [0, 2\pi]$ with start $s_1 = (0, 0, 0)$. (b) Lattice \mathcal{X} as in (a) with start set $\mathcal{S} = [s_0 = (0, 0, 0), s_1 = (0, 0, \pi/4)]$.

are many examples of configuration spaces for which a single start is insufficient to capture the full variety of motions. For example, let

$$\begin{aligned} \mathcal{X} &= \mathbb{R}^2 \times [0, 2\pi], \\ L &= \mathbb{Z}^2 \times \{i\pi/4, i = 0, \dots, 7\}, \\ s_0 &= (0, 0, 0), \end{aligned}$$

denote configurations space, lattice, and starting vertex, respectively – as in Figure 3 (a). Observe that if $i = (1, 1, \pi/4) \in L$ and $j = (2, 2, \pi/4) \in L$, then the motion p_0 from i to j is such that $s_0 \cdot p_0 \notin L$. Therefore, p_0 will not appear in any action set E and no concatenations of motions in any E will produce a simple diagonal motion. This may result in zig-zag motions along diagonal lines. A naive approach to compensate is to augment the lattice vertices to include those configurations obtained by all possible concatenations. However, this may result in prohibitively large lattices nullifying the benefits of the discretization.

We propose a different solution by way of a multi-start Lattice. Given a set of starts $\mathcal{S} \subset L$, vertices $i, j \in L$ and motion p from i to j , we say that $i \cdot p$ is a *valid concatenation*, and write $i \oplus p$ if there exists a start $s \in \mathcal{S}$ such that $s \cdot p \in L$. In the example in Figure 3 (b), let $\mathcal{S} = [s_0 = (0, 0, 0), s_1 = (0, 0, \pi/4)]$, let p_1 be the motion from s_0 to i , and let p_2 be the motion from s_1 to i . Then, observe that $i \oplus p_2 = j$ is a valid concatenation. Moreover, $s_0 \oplus p_1 \oplus p_2 = j$ is a string of valid concatenations resulting in a motion from s_0 along a diagonal to j .

The goal is to produce a set of starts \mathcal{S} such that for every pair of vertices $i, j \in L$ with motion p from i to j , the concatenation $i \cdot p$ is valid. This is simple for a certain class of configuration spaces described here. For motion planning for autonomous cars and car-like robots, we typically use a configuration space of the form

$$\mathcal{X} = \mathbb{R}^2 \times [0, 2\pi) \times U_0 \cdots \times U_N, \quad (1)$$

where $(x, y) \in \mathbb{R}^2$ represents the planar location of the vehicle, $\theta \in [0, 2\pi)$ the heading, and $U_i \subseteq \mathbb{R}$ higher order states for $i = 0 \dots N$. Typical higher order states include curvature κ , curvature rate σ , velocity v , and longitudinal acceleration a . For such a configuration space, we construct a lattice $L \subseteq \mathcal{X}$ by discretizing each state separately. In particular, for $\alpha, \beta \in \mathbb{R}_{>0}$, and $n_0, n_1, n_2, m_i \in \mathbb{N}$ for $i = 0 \dots N$, we let

$$\begin{aligned} L = & \{i\alpha, i = -n_0 \dots n_0\} \\ & \times \{i\beta, i = -n_1 \dots n_1\} \\ & \times \{\pi i / 2^{n_2-1}, i = 0 \dots 2^{n_2} - 1\} \\ & \times \prod_{i=0}^N \{U_i^0 + j/m_i, j = 0 \dots (U_i^1 - U_i^0)m_i\}. \end{aligned} \quad (2)$$

This lattice samples $2n_0 + 1$, and $2n_1 + 1$ values of the x, y coordinates, respectively, with spacing α, β between samples, respectively. We also partition the heading space $[0, 2\pi)$ into 2^{n_2} evenly spaced samples. Finally, we assume that for all $i = 0 \dots N$, $U_i = [U_i^0, U_i^1] \subseteq \mathbb{R}$ which we partition into m_i evenly spaced samples. For such a configuration space and state lattice, we let

$$\begin{aligned} \mathcal{S} = & \left\{ (0, 0, \theta, u_0, \dots, u_N) : \right. \\ & \theta \in \{j\pi / 2^{n_2-1}, j = 0, \dots, 2^{n_2-2} - 1\}, \\ & \left. u_i \in \{U_i^0 + j/m_i, j = 0 \dots (U_i^1 - U_i^0)m_i\} \right\}. \end{aligned} \quad (3)$$

We observe that given a configuration space \mathcal{X} , and lattice L defined as above, it holds that for any vertices $i, j \in L$, the motion p from i to j is such that $\exists s \in \mathcal{S}$ with $s \oplus p \in L$.

In the next section, we describe how multi-start lattices can be used in motion planning, and we formulate the multi-start Minimum t -Spanning Control Set (MTSCS) problem that is the focus of this paper.

B. Path Planning with a Multi-Start Control Set

In this section, we describe how multi-start lattices can be used in motion planning. In this work, we assume that for all $i, j \in \mathcal{X}$, there exists a motion p solving problem II.1 from i to j in the absence of obstacles. We assume further that the cost of this motion $c(p)$, is known, non-negative, obeys the triangle inequality, and is equal to 0 if and only if $i = j$. This cost is left general, and may represent arc-length, travel time, integral of the squared jerk, etc.

The high level idea is the following: given the tuple $(\mathcal{X}, L, \mathcal{S}, c)$ of configuration space, lattice, starting set, and cost of motions between lattice vertices, respectively, we pre-compute a cost-minimizing feasible motion between each configuration $s \in \mathcal{S}$, and each vertex $i \in L - \mathcal{S}$ in the absence of obstacles. Let \mathcal{B}_s denote the set of all such motions, and $\mathcal{B} = \bigcup_{s \in \mathcal{S}} \mathcal{B}_s$. We then compute a subset $E \subseteq \mathcal{B}$ of optimal feasible motions which we use as an action set during an online search in the presence of obstacles. In particular, for each $s \in \mathcal{S}$, we compute a subset $E_s \subseteq \mathcal{B}_s$ representing the action set at s , and let $E = \bigcup_{s \in \mathcal{S}} E_s$. As discussed in the previous section, not all motions in E will result in valid concatenations. This gives rise to the following definition:

Definition II.2 (Relative start). Given a tuple $(\mathcal{X}, L, \mathcal{S})$, and a vertex $i \in L$, the *relative start* of i is the configuration

$R(i) \in \mathcal{S}$ such that for each $j \in L$, the motion p_j from s to j is such that $i \oplus p_j$ is a valid concatenation.

Intuitively, the relative start of $i \in L$, is the $s \in \mathcal{S}$ that is *most like* i . If L, \mathcal{S} are given by (2), (3), respectively, then the relative start of any configuration $i = (x, y, \theta, u_1, \dots, u_N) \in L$ is $R(i) = (0, 0, \theta', u_1, \dots, u_N)$ where

$$\theta' = \frac{\pi}{2^{n_2-1}} \left(\left(\frac{2^{n_2-1}\theta}{\pi} \right) \bmod 4 \right).$$

The set of available motions during an online search – i.e., the action set – at a configuration $i \in L$ is given by

$$M(i) = E_{R(i)},$$

and the cost of each motion $p \in M(i)$ is given by $c(p)$. By using $M(i)$ as the set of available motions at i , we ensure that $i \oplus p$ is indeed a valid concatenation for each $p \in M(i)$ by definition of the relative start.

For any subset $E \subseteq \mathcal{B}$, we denote by \bar{E} the set of all tuples $(i, j) \in L^2$ such that if p is the optimal feasible motion from i to j , then $p \in E_{R(i)}$. Summarizing notation:

$$\begin{aligned} \mathcal{B}_s &= \{p : \exists i, j \in L, i \oplus p = j\}, \quad \forall s \in \mathcal{S} \\ E_s &\subseteq \mathcal{B}_s, \quad \forall s \in \mathcal{S} \\ E &= \bigcup_{s \in \mathcal{S}} E_s, \quad \mathcal{B} = \bigcup_{s \in \mathcal{S}} \mathcal{B}_s \\ \bar{E} &= \{(i, j) \in L^2 : (i \oplus p = j) \Rightarrow p \in E_{R(i)}\}. \end{aligned} \quad (4)$$

Intuitively, \bar{E} represents the set of edges in a directed graph whose vertex set is L , and such that two vertices i, j are connected by an edge if the optimal feasible motion from i to j is isometric to a motion in $E_{R(i)}$ – the action set at the relative start of i .

Computing a motion between lattice vertices is equivalent to computing a shortest path in the weighted directed graph $G = (L, \bar{E}, c)$. For edge $(i, j) \in \bar{E}$, the cost of the edge $c((i, j))$ is defined as the cost of the optimal feasible motion from i to j .

The above illustrates how a set E – called a *control set* – of the motions can be used in motion planning. The question now is: how should E be computed? Ideally, E is such that the set of available motions $E_{R(i)}$ at any vertex i is small in order to limit the branching factor during an online search, but costs of paths in the graph G are close to optimal. In order to evaluate the quality of an action set E , we present two definitions:

Definition II.3 (Path using E). Given the tuple $(\mathcal{X}, L, \mathcal{S}, c, E)$, the *path using* E from $s \in \mathcal{S}$ to $j \in L$, denoted $\pi^E(s, j)$ is the cost-minimizing path from s to j (ties broken arbitrarily) in the absence of obstacles in the weighted, directed graph $G = (L, \bar{E}, c)$.

Definition II.4 (Motion cost using E). Given the tuple $(\mathcal{X}, L, \mathcal{S}, c, E)$, the cost of a motion *using* E from $s \in \mathcal{S}$ to $j \in L$, denoted $d^E(s, j)$ is the cost of the path using E from s to j .

Observe that if $E = \mathcal{B}$, that is, if E is the set of *all* cost-minimizing feasible motions from all $s \in \mathcal{S}$ to all $i \in L$, then $\pi^E(s, j) = p$, and $d^E(s, j) = c(p)$ where p is the cost-minimizing feasible motion from s to j . Therefore,

$$\begin{aligned} \pi^{\mathcal{B}}(s, j) &= p, \\ d^{\mathcal{B}}(s, j) &= c(p). \end{aligned}$$

This implies that using \mathcal{B} as a control set will result in paths with minimal cost. However, because \mathcal{B} can be large the branching factor at a vertex $i \in L$ during an online search – given by $|M(i)|$ – may be prohibitively large. We therefore wish to limit the size of $|M(i)|$ in such a way that does not overly adversely affect $d^E(s, j)$ for all $j \in L$. This motivates the following definition:

Definition II.5 (*t*-Error). Given the tuple $(\mathcal{X}, L, \mathcal{S}, c, E)$, the *t*-error of E is defined as

$$tEr(E) = \max_{\substack{s \in \mathcal{S} \\ j \in L-S}} \frac{d^E(s, j)}{d^{\mathcal{B}}(s, j)}.$$

That is, the *t*-error of a control set E is the worst-case ratio of the distance using E from a start s to a vertex j to the cost of the optimal path from s to j taken over all starts s and vertices j in the lattice. The notion of the *t*-Error motivates the following definition augmented from [7] to account for a multi-start lattice:

Definition II.6 (*t*-Spanning Set). Given the tuple $(\mathcal{X}, L, \mathcal{S}, c, E)$, and a real number $t \geq 1$, we say that a set E is a *t*-spanner of L (or *t*-spans L), if $tEr(E) \leq t$.

Our objective is to compute a control set E that optimizes a trade-off between branching factor and motion quality. This is formulated in the following problem:

Problem II.7 (Multi-Start *t*-spanning Control Set Problem).

Input: A tuple $(\mathcal{X}, L, \mathcal{S}, c)$, and a real number $t \geq 1$.

Output: A control set $E = \bigcup_{s \in \mathcal{S}} E_s$ that *t*-spans L where $\max_{s \in \mathcal{S}} |E_s|$ is minimal.

This strategy has two beneficial properties. First, because the number of available actions $|M(i)| = |E_{R(i)}|$ for all $i \in L$ (where $R(i)$ is the relative start of i), and $\max_{s \in \mathcal{S}} |E_s|$ is minimized, the branching factor during an online search is kept small. Second, observe that if E is a solution to Problem II.7, then for every $j \in V$ and every $s \in \mathcal{S}$, it must hold that $d^E(s, j) \leq tc(s, j)$. Thus, Problem II.7 represents a trade-off between branching factor and motion quality.

III. MAIN RESULTS

In this section we present a MILP reformulation of Problem II.7, and algorithms to compute and smooth motions using the control sets returned by Problem II.7.

A. Multi-Start MTSCS Problem: MILP Formulation

Begin by noting that Problem II.7 is NP-hard. Indeed, if $|\mathcal{S}| = 1$, then the problem was shown to be NP-hard in [7]. Moreover, we observe that there is a trivial reduction from Problem II.7 when $|\mathcal{S}| = 1$ to Problem II.7 where $|\mathcal{S}| \geq 1$. Therefore, we are motivated to provide a MILP formulation of Problem II.7.

Consider the tuple $(\mathcal{X}, L, \mathcal{S}, c)$ of configuration space, lattice, start set, and cost of vertex-to-vertex motions in L , respectively. As above, for each starting configuration $s \in \mathcal{S}$, let \mathcal{B}_s denote the set of all cost-minimizing feasible motions from s to each $i \in L$, and let $\mathcal{B} = \bigcup_{s \in \mathcal{S}} \mathcal{B}_s$. Finally, for any motion $q \in \mathcal{B}$, let

$$S_q = \{(i, j) : i, j \in L, i \oplus q = j\}.$$

That is, S_q is the set of all pairs $(i, j) \in L^2$ such that q is a cost-minimizing feasible motion from i to j and $i \cdot q$ is a valid concatenation. Observe that by definition of a valid concatenation, there must exist a start $s \in \mathcal{S}$ and vertex $j' \in L$ such that q is a motion from s to j' implying that $(s, j') \in S_q$.

Let $E = \bigcup_{s \in \mathcal{S}} E_s$ be a solution to Problem II.7. Let $G = (L, \bar{E}, c)$ be the weighted directed graph with edges \bar{E} given in (4). For each $s \in \mathcal{S}$ and each $(i, j) \in \bar{E}$, we make a copy $(i, j)^s$ of the edge. This allows us to treat edges differently depending on the starting vertex of the path to which they belong. Observe that for each $r \in L$, a path using E from s to r (that is, $\pi^E(s, r)$) may be expressed as a sequence of edges $(i, j)^s$ where $(i, j) \in E$. Motivated by this observation, for each $s \in \mathcal{S}$ we construct a new graph

$$T^s = (L, E_T^s), \quad (5)$$

whose edges E_T^s are defined as follows: let

$$T^{s'} = \bigcup_{i \in L-S} \pi^E(s, i).$$

Thus $T^{s'}$ is the set of all minimal cost paths from s to vertices $i \in L - S$ in the graph G . These paths are expressed as a sequence of edge copies $(i, j)^s$ where $(i, j) \in \bar{E}$.

For each $i \in L - S$, and for each $s \in \mathcal{S}$, if $T^{s'}$ contains two paths π_1^E, π_2^E taking s to i , determine the last common vertex j in paths π_1^E, π_2^E , and delete the the copy of the edge in π_2^E whose endpoint is j from $T^{s'}$. Let the remaining edges be the set E_T^s . The graph T^s has a property that facilitates the development of a MILP reformulation of Problem II.7. We begin with a definition.

Definition III.1 (Arborescence). From Theorem 2.5 of [29], a graph T with a vertex s is an arborescence rooted at s if every vertex in T is reachable from s , but deleting any edge in T destroys this property.

The graph T^s for each $s \in \mathcal{S}$ is in fact an arborescence rooted at s . This is shown in the following Lemma:

Lemma III.2 (Multi-Start Arborescence). *Let $E = \bigcup_{s \in \mathcal{S}} E_s$ be a solution to Problem II.7. Let $G = (L, \bar{E}, c)$ be the weighted directed graph with edges \bar{E} given in (4). For each $s \in \mathcal{S}$, if T^s is given by (5), then T^s is an arborescence rooted at s , and the distance using E from s to i , $d^E(s, i)$ is the length of the path in T^s to i .*

Proof. Let $s \in \mathcal{S}$. To show that T^s is an arborescence rooted at s , observe first that there is a path in T^s from s to all $i \in L$. Indeed, if E solves Problem II.7, then E *t*-spans L . In particular, there must be at least one path, $\pi^E(s, i)$ using E from s to each $i \in L$ implying that $\pi^E(s, i) \in T^{s'}$. Since E_T^s only deletes duplicate paths from $T^{s'}$, there must still be a path in T^s from s to i . Furthermore, by construction of the edge set E_T^s , duplicate paths (with equal cost) are deleted thus ensuring the uniqueness of paths from s to each $i \in L$ completing the proof that T^s is an arborescence rooted at s . Finally, the cost of the path in T^s from s to i is defined as the cost of the path $\pi^E(s, i)$ which is the distance in E from s to i by definition. \square

Lemma III.2 implies that E is a *t*-spanner of L if and only if $\forall s \in \mathcal{S}$ there is a corresponding arborescence T^s rooted

at s whose vertices are L , whose edges $(i, j)^s$ are copies of members of S_q for some $q \in E$, and such that the cost of the path from s to any vertex $i \in L$ in T^s is no more than a factor of t from the optimal path from s to i . Indeed, the forward implication follows from Lemma III.2, while the converse holds by definition of a t -spanner. From this, we develop four criteria that represent necessary and sufficient conditions for E to be a t -spanning control set of L :

Usable Edge Criteria: For any $q \in \mathcal{B}$, for any $s \in \mathcal{S}$, and for any $(i, j) \in S_q$, the copy $(i, j)^s$ may belong to a path in T^s from s to a vertex $r \in L$ if and only if $q \in E_s$.

Cost Continuity Criteria: For any $s \in \mathcal{S}$, $q \in \mathcal{B}$, $(i, j) \in S_q$, and $(i, j)^s$, if $(i, j)^s$ then the path in T^s to vertex j contains vertex i . Thus $c(\pi^E(s, j)) = c(\pi^E(s, i)) + c(q)$. That is, the cost of the path from s to j in T^s is equal to the cost of the path from s to i plus the cost of the motion from i to j .

t -Spanning Criteria: The length of the path in T^s to any vertex $j \in L - \mathcal{S}$ can be no more than t times the length of the direct motion from s to j .

Arborescence Criteria: The set T^s must be an arborescence for all $s \in \mathcal{S}$.

We now present how to encode these four criteria. Let $|L| = n$ and all the vertices are enumerated as $1, 2, \dots, n$ with $s \in \mathcal{S}$ taking the values $1, \dots, m$ for $m \leq n$. For any control set $E \subseteq \mathcal{B}$ where $E = \bigcup_{s \in \mathcal{S}} E_s$, define $m(n - m - 1)$ decision variables $y_q^s, q = m + 1, \dots, n$

$$y_q^s = \begin{cases} 1, & \text{if } q \in E_s \\ 0, & \text{otherwise.} \end{cases}$$

For each edge $(i, j) \in \bar{\mathcal{B}}$, and each $s \in \mathcal{S}$ let

$$x_{ij}^s = \begin{cases} 1 & \text{if } (i, j)^s \in T^s \\ 0 & \text{otherwise.} \end{cases}$$

That is, $x_{ij}^s = 1$ if $(i, j)^s$ (the copy of the edge (i, j) for start $s \in \mathcal{S}$) lies on a path from s to a vertex in the lattice. Let z_i^s denote the length of the path in the tree T^s to vertex i for any $i \in L$, c_{ij} the cost of the optimal feasible motion from i to j , and let $L' = L - \mathcal{S}$. We now modify the mixed integer linear programming formulation proposed in [7] to account for a starting set \mathcal{S} of possibly non-unit size:

$$\min K \quad (6a)$$

$$s.t. \forall s \in \mathcal{S} \quad (6b)$$

$$y_q^s \leq K, \quad \forall q \in \mathcal{B} \quad (6c)$$

$$x_{ij}^s - y_q^s \leq 0, \quad \forall (i, j) \in S_q, \forall q \in \mathcal{B} \quad (6d)$$

$$z_i^s + c_{ij} - z_j^s \leq M_{ij}^s(1 - x_{ij}^s), \quad \forall (i, j) \in \bar{\mathcal{B}} \quad (6e)$$

$$z_j^s \leq tc_{sj}, \quad \forall j \in L' \quad (6f)$$

$$\sum_{i \in L'} x_{ij}^s = 1, \quad \forall j \in L' \quad (6g)$$

$$x_{ij}^s \in \{0, 1\}, \quad \forall (i, j) \in \bar{\mathcal{B}} \quad (6h)$$

$$y_q^s \in [0, 1], \quad \forall q \in \mathcal{B}, \quad (6i)$$

where $M_{ij}^s = tc_{si} + c_{ij} - c_{sj}$. The objective function (6a) together with constraint (6c) minimizes $\max_{s \in \mathcal{S}} |E_s|$ as in Problem II.7. The remainder of the constraints encode the four criteria guaranteeing that E is a t -spanning set of L :

Constraint (6d): Let q be the motion in \mathcal{B} from s to $j \in L$. If $q \notin E_s$, then $y_q^s = 0$ by definition. Therefore, (6d) requires that $x_{ij}^s = 0$ for all $(i, j) \in S_q$. Alternatively, if $y_q^s = 1$, then x_{ij}^s is free to take values 1 or 0 for any $(i, j) \in S_q$. Thus constraint (6d) encodes the Usable Edge Criteria.

Constraint (6e): Constraint (6e) takes a similar form to [30, Equation (3.7a)]. Note that $M_{ij}^s \geq 0$ for all $(i, j) \in \mathcal{B}$. Indeed, $\forall t \geq 1, M_{ij}^s \geq c_i + c_{ij} - c_j$, and $c_i + c_{ij} \geq c_j$ by the triangle inequality. Replacing the definition of M_{ij}^s in (6e) yields

$$z_i^s + c_{ij} - z_j^s \leq (tc_i + c_{ij} - c_j)(1 - x_{ij}^s). \quad (7)$$

If $x_{ij}^s = 1$, then $(i, j)^s$ is on the path in T^s to vertex j and (7) reduces to $z_j^s \geq z_i^s + c_{ij}$ which encodes the Cost Continuity Criteria. If, however, $x_{ij}^s = 0$, then (7) reduces to $z_i^s - z_j^s \leq tc_i - c_j$ which holds trivially by constraint (6f) and by noting that $z_j^s \geq c_j, \forall j \in L$ by the triangle inequality.

Constraint (6g): Constraint (6g) together with constraint (6e) yield the Arborescence Criteria. Indeed for all $s \in \mathcal{S}$, by Theorem 2.5 of [29], T^s is an arborescence rooted at s if every vertex in T^s other than s has exactly one incoming edge, and T^s contains no cycles. The constraint (6g) ensures that every vertex in L' , which is the set of all vertices in T^s other than those in \mathcal{S} , have exactly one incoming edge, while constraint (6e) ensures that T^s has no cycles. To see why this is true, suppose that a cycle existed in T^s , and that this cycle contained vertex $i \in L'$. Suppose that this cycle is represented as

$$i \rightarrow j \rightarrow \dots \rightarrow k \rightarrow i.$$

Recall that it is assumed that the cost of any motion between two different configurations in \mathcal{X} is strictly positive. Therefore, (6e) implies that $z_i^s < z_j^s$ for any $(i, j) \in \bar{\mathcal{B}}$. Therefore,

$$z_i < z_j < \dots < z_k < z_i,$$

which is a contradiction.

Constraint (6i): For all $s \in \mathcal{S}, q \in \mathcal{B}$, the variable y_q^s is a decision variable, and therefore should take values in $\{0, 1\}$. However, the integrality constraint on y_q^s may be relaxed to (6i). Indeed, suppose that for any $q \in \mathcal{B}$, there exists an edge $(i, j) \in S_q$ such that $x_{ij}^s = 1$. Then, by (6d), $y_q^s \geq 1$ which implies by (6i), that $y_q^s = 1$. If, on the other hand, there does not exist $(i, j) \in S_q$ with $x_{ij}^s = 1$, then y_q^s is free to take values in $[0, 1]$. Therefore, $y_q^s = 0$ as the objective function seeks to minimize the size of the maximum control set.

B. Motion Planning With a MTSCS

The previous section illustrates how to compute a control set $E = \bigcup_{s \in \mathcal{S}} E_s$ given the tuple $(\mathcal{X}, L, \mathcal{S}, c)$ for a multi-start lattice L . Moreover we have presented a high-level description of how such a control set may be used during an online A*-style search of the weighted directed graph $G = (L, \bar{E}, c)$ where the edge set \bar{E} is the set of pairs $(i, j) \in L^s$ such that there exists a motion $p \in E_{R(i)}$ from i to j where $R(i) \in \mathcal{S}$ is the relative start of i . The motion primitives in this control set could be used in any graph-search algorithm, and could be used to replace existing motion primitives in work like [19]. In this section, we propose one such algorithm: an A* variant, *Primitive A* Connect* (PrAC) for path computation in G . The

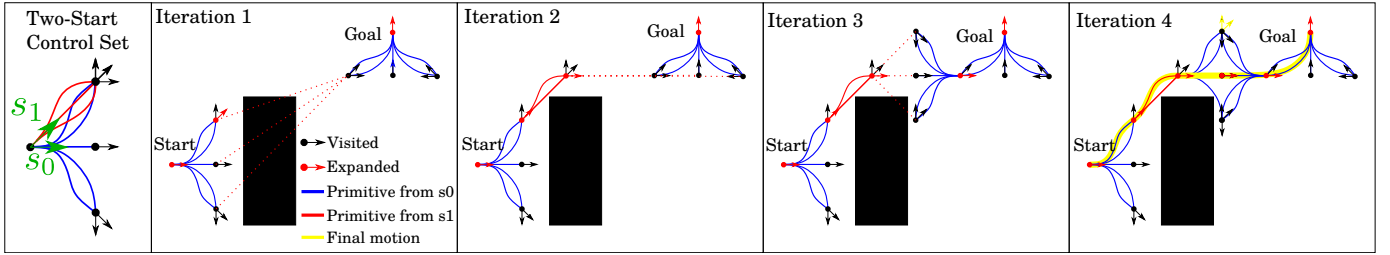


Fig. 4: Example motion planning using PrAC for a 2-start lattice.

algorithm follows the standard A* algorithm closely with some variations described here:

Tunable Cost: In the standard A* algorithm, two costs are for each vertex i are maintained: the value $g(i)$ represents the current minimal cost to reach vertex i from the starting vertex x_s , while $f(i) = g(i) + h(i)$ represents the estimated cost to reach the goal vertex x_g by passing through i given heuristic h . At each iteration, the current expanded vertex is the one that minimizes f over all vertices in an open set. Thus equal weight is placed on the *cost to get* to each vertex, $g(i)$, and the *cost to go* from this vertex to x_g , $h(i)$.

We implement a new weighting system: Given a value $\lambda \in [0, 1]$, we let $a = 0.5\lambda$, $b = 1 - 0.5\lambda$, and we define a new cost function $f' = ag(i) + bh(i)$. If $\lambda = 1$, then both cost to get and cost to go are weighted equally, resulting in the standard A* algorithm. However, as λ approaches 0, more weight is placed on the cost to go resulting in expanding vertices with smaller heuristic values which promotes *exploration* over *optimization*. While using a value $\lambda < 1$ eliminates optimality guarantees, it also empirically improves runtime performance. Moreover, it has been found empirically that optimality is often reclaimed once the path is smoothed. In practice, using $\lambda = 1$ works well for maneuvers where x_s and x_g are close together, like parallel parking, while small values of λ work well for longer maneuvers like traversing a parking lot.

Observe that setting $\lambda = 0$ results in an algorithm which expands those vertices which maximally take the current vertex to the goal. This is a technique used often in motion planning on highways [22].

Expanding Start and Goal Vertices: Similar to the RRT-connect algorithm in [31], we expand vertices neighboring both start and goal vertices and attempt to connect these vertices on each iteration. In particular, we maintain two trees, one rooted at the start vertex x_s , denoted T_{x_s} , the other at the goal, denoted T_{x_g} . On each iteration of the A* while loop, we expand a vertex v in T_{x_s} by applying available motions in $E_{R(v)} \cup \{p\}$ where $E_{R(v)}$ is the set of available motions at the relative start of v , and p is a motion taking v to the "closest" vertex in T_{x_g} . By "closest", we mean relative to a heuristic. In the same iteration, we then swap T_{x_s} and T_{x_g} and perform the same steps but with all available motions in reverse. This is illustrated in Figure 4. Critically, observe that because all available motions at any vertex take lattice vertices to lattice vertices, all vertices of both T_{x_s}, T_{x_g} will be in L . Therefore, computing p – the motion from the current vertex v to the closest vertex in the opposite tree – is trivial, as all lattice motions in \mathcal{B} have been pre-computed. Expanding start and goal vertices has proven especially useful during complex

maneuvers like backing into a parking space.

Augmented Heuristic: Because we are expanding two trees T_{x_s}, T_{x_g} simultaneously, a basic heuristic which returns an estimated cost from a current vertex to a goal is no longer applicable. Given an A*-admissible heuristic h' , we perform an augmentation to a function h which can be used in our modified algorithm. Let O_{x_s}, O_{x_g} denote the vertices in T_{x_s}, T_{x_g} , respectively, that have been visited but not yet expanded, then

$$h(v) = \begin{cases} \min_{u \in O_{x_g}} h'(v, u) & \text{if } v \in T_{x_s} \\ \min_{u \in O_{x_s}} h'(u, v) & \text{if } v \in T_{x_g}. \end{cases} \quad (8)$$

The value of u that is the minimum argument in h' is the "closest" vertex described in the Expanding Start and Goal Vertices description.

Off-lattice Start and Goal Vertices: It is very likely that the start and goal vertices, x_s, x_g do not lie in a lattice. Further, newly discovered obstacles, or excessive noise in the system may require a new motion to be planned from a configuration that does not lie in the original lattice. As a result, x_s, x_g may have no relative start and therefore no available actions. Similar to the re-planning technique in [5], we use lattices with graduated fidelity. In particular, for a lattice given by (2) with values n_0, n_1, n_2 and $m_i, i = 0, \dots, N$, we compute a control set E^1 using the MILP in (6). Next we compute a control set E^2 for a lattice with a much finer start set (we found that increasing $m_i, i = 0, \dots, N$ by a factor of 10, and setting $n_2 = n_2 + 2$ works well). The non-start vertices of this latter lattice are left the same as the original lattice, but the fidelity of the start set is increased to account for off-lattice starts/goals. The set of available actions from start-goal pair that do not have any available motions in the control set E^1 will have available motions in E^2 (for sufficiently large values of n_2, m_i), and these motions will bring the start and goal configurations to the lower-fidelity lattice on which control set E^1 may plan the remaining motion. (6).

C. Motion Smoothing

Given the tuple $(\mathcal{X}, L, \mathcal{S}, c, E)$, of configuration space, lattice, cost function, and MTSCS, respectively, let $G = (L, \bar{E}, c)$ be the weighted directed graph described above with edge set \bar{E} given in (4).

We now present a smoothing algorithm based on the *shortcut* approach that takes as input a path in E , here $\pi^E(x_s, x_g)$, between start and goal configurations x_s, x_g . This path is expressed as a sequence of edges in G . Thus, $\pi^E(x_s, x_g) = \{(i_r, i_{r+1}), r = 1, \dots, m - 1\}$ for some $m \in \mathbb{N}_{\geq 2}$ where

$(i_r, i_{r+1}) \in \bar{E}$ for all $r = 1, \dots, m-1$ and $i_1 = x_s, i_m = x_g$. Let C_π denote the set of all configurations along motions p from i_r to i_{r+1} for all $(i_r, i_{r+1}) \in \pi^E(x_s, x_g)$. Algorithm 1 summarizes the proposed approach.

Algorithm 1 Smoothing Lattice Path

```

1: procedure DAGSMOOTH( $\pi^E(x_s, x_g), C_\pi, \mathcal{X}_{\text{obs}}, c, n, \Psi$ )
2:    $V_1 \leftarrow \text{SampleRandom}(n, C_\pi)$ 
3:    $V \leftarrow \{i_r\}_{r=1}^m \cup V_1$  in the order that they appear in  $C_\pi$ 
4:    $\{j_r\}_{r=1}^{m+n} \leftarrow V$ 
5:   for  $j \in V$  do
6:      $\text{dist}(j) = \infty$ 
7:    $\text{dist}(j_1) = 0$ 
8:    $\text{Pred}(j_1) = \text{None}$ 
9:   for  $u$  from 1 to  $n + m - 1$  do
10:    for  $v$  from  $u + 1$  to  $m + n$  do
11:       $p_1 = \text{motion from } j_u \text{ to } j_v$ 
12:       $p_2 = \text{motion from } j_v \text{ to } j_u$ 
13:       $c = \min(c(p_1), \psi(c(p_2)))$ 
14:       $p = \arg \min(c(p_1), \Psi(c(p_2)))$ 
15:      if  $\text{dist}(j_u) + c \leq \text{dist}(j_v)$  then
16:        if  $\text{CollisionFree}(p, \mathcal{X}_{\text{obs}})$  then
17:           $\text{dist}(j_v) = \text{dist}(j_u) + c$ 
18:           $\text{Pred}(j_v) = j_u$ 
return Backwards chain of predecessors from  $i_m$ 

```

Algorithm 1 takes as input a collision-free, dynamically feasible path π^E between start and goal configurations – such as that returned by PrAC – as well as the set of all configurations C_π , a set of obstacles \mathcal{X}_{obs} , a cost function of motions c , and a non-negative natural number n . It also takes a function $\Psi : \mathbb{R} \rightarrow \mathbb{R}$ which is used to penalize reverse motion. That is, given two configurations $i, j \in \mathcal{X}$ with a motion p from i to j , we say that the cost of the motion p is $c(p)$, while the cost of the reverse motion p' from j to i that is identical to p but traversed backwards is $c(p') = \Psi(c(p))$.

The set V in Line 3 represents sampled configurations along the set of configurations C_π . This sample includes all endpoints of the edges $(i_r, i_{r+1}) \in \pi^E$, as well as n additional random configurations along motions connecting these endpoints. Critically, configurations in V must be in the order in which they appear along π^E .

Were we to form a graph with vertices V and with edges $(j_u, j_v) \in V^2$ where j_v occurs farther along C_π than j_u and where the optimal feasible motion from j_u to j_v is collision-free, then observe that this graph would be a directed, acyclic graph (DAG). Indeed, were this graph not acyclic, then the path $\pi^E(x_s, x_g)$ would contain a cycle implying that a configuration would appear at least twice in $\pi^E(x_s, x_g)$. This is impossible by construction of the PrAC algorithm which maintains two trees rooted at x_s, x_g , respectively. Observe further that the cost of the motion from j_u to j_v is given by Line 13 of the Algorithm. Indeed, for forward motion of the vehicle, we compute the cost from j_u to j_v , while for reverse motion, we can compute the cost from j_v to j_u . If $c = \Psi(c(p_2))$, then the motion from j_v to j_u traversed backwards from j_u to j_v is used. This motivates the following observation:

Observation III.3. *The nested for loop in lines 9-10 of Algorithm 1 are constructing a directed, weighted, acyclic graph and solving the minimum path problem from x_s to x_g on that graph.*

This observation motivates the following theorem

Theorem III.4. *Let π_1^E be the input path to Algorithm 1 between configurations x_s, x_g with cost $c(\pi_1^E)$. Let π_2^E be the path returned by Algorithm 1 with cost $c(\pi_2^E)$. Then $c(\pi_2^E) \leq c(\pi_1^E)$. Moreover, if $n = 0$, this algorithm runs in time quadratic in the number of vertices along π_1^E .*

Proof. By Observation III.3, Algorithm 1 constructs a DAG containing configurations x_s, x_g as vertices. It also solves the minimum cost path problem on this DAG. Observe further that by construction of the DAG vertex set in Line 3, all configurations along the original path π_1^E are in V . Thus π_1^E is an available solution to the minimum path problem on the DAG. This proves that the minimum cost path can do no worse than $c(\pi_1^E)$. If $n = 0$, then V is the set of endpoints of edges in π_1^E . Therefore, $V \subseteq L$. Because all motions between lattice vertices have been pre-computed in \mathcal{B} , Lines 11,12 can be executed in constant time, and the nested for loop in lines 9-10 will thus run in time $O(m)^2$ where m is the number of vertices on the path π_1^E . \square

IV. RESULTS

We verify our proposed technique against two techniques in two common navigational settings. The techniques described here were encoded in Python 3.7 (Spyder). Results were obtained using a desktop equipped with an AMD Ryzen 3 2200G processor and 8GB of RAM running Windows 10 OS. Start and goal configurations were not constrained to be lattice vertices. We assume that all obstacles are known to the planner ahead of time, and that the environment is noiseless. As such, the results that follow can be thought of as a single iteration of a full re-planning process.

A. Memory

In order to keep required memory low, all pre-computed motions are stored, not as a set of configurations, but as the smallest amount of information required to easily generate those configurations. In particular, the motions used in this section are $G3$ curves which take the form CCC, or CSC where "C" denotes a curved segment, and "S" a straight segment. Such motions can be easily generated by storing the maximum curvature obtained in each segment [32]. Thus instead of storing all configurations along a motion, we store only three values. Similarly, a velocity profile can be re-computed by saving very few (we use 7) values of acceleration along the motion [32].

B. Parking Lot Navigation

We begin by validating the proposed method against a common technique: Hybrid A* [2] in a parking lot scenario. In [33], the authors present a method of computing paths comprised of $G3$ curves under certain simplifying assumptions. In [32], we extend this work by removing these assumptions. In particular, we present a method of computing motions

between start and goal configurations in the configurations space $\mathcal{X} = \mathbb{R}^2 \times [0, 2\pi) \times \mathbb{R}^3$. Here, configurations take the form $(x, y, \theta, \kappa, \sigma, \rho)$ where (x, y, θ) represent the planar coordinates and heading of a vehicle, κ the curvature, σ the curvature rate (defined as $d\kappa/ds$ for arc-length s), and ρ the second derivative of curvature with respect to arc-length. In [32], we generate motions with continuously differentiable curvature profiles assuming that κ, σ, ρ are bounded in magnitude. The motivation for this work comes from the observation that jerk, the derivative of acceleration with respect to time, is a known source of discomfort for the passengers of a car [21]. In particular, minimizing the integral of the squared jerk is often used a cost function in autonomous driving [22]. Since this value varies with σ , keeping σ low and bounded is desirable in motion planning for autonomous vehicles.

Unfortunately, due to the increased complexity of the configuration space over, say, the configuration space used in the development of Dubins' paths, $\mathcal{X}_{\text{Dubins}} = \mathbb{R}^2 \times [0, 2\pi)$, solving TPBV problems in \mathcal{X} takes on average two orders of magnitude more time than computing a Dubins' path. Though motions computed using the techniques in [33], [32] are more comfortable, and result in lower tracking error than Dubins' paths, they may be computationally impractical to use in motion planners that require solving many TPBV problems online. However, they prove to be particularly useful in the development of pre-computed motion primitives.

1) *Lattice Setup & Pruning*: The configuration space used here is $\mathcal{X} = \mathbb{R}^2 \times [0, 2\pi) \times \mathbb{R}^3$ with configurations $(x, y, \theta, \kappa, \sigma, \rho)$. Motion primitives were generated using the MILP in (6) for a 15×20 square lattice with 16 headings and 3 curvatures, and a value of $t = 1.1$ (10% error from optimal). To account for the off-lattice start-goal pairs, we used a higher-fidelity lattice with 64 headings and 30 curvatures. Lattice vertex values of σ, ρ were set to 0. This results in a start set \mathcal{S} with 12 starts given by (3). The cost c of a motion is defined by the arc-length of that motion. These motions were computed using our work in [32] with bounds on κ, σ, ρ :

$$\kappa_{\max} = 0.1982m^{-1}, \quad \sigma_{\max} = 0.1868m^{-2}, \quad \rho_{\max} = 0.3905m^{-3}. \quad (9)$$

that were deemed comfortable for a user [33], particularly at low speeds typical of parking lots. The spacing of the lattice x, y -values was chosen to be $r_{\min}/4$ for a minimum turning radius $r_{\min} = 1/\kappa_{\max}$. Finally, if the cost of the motion from $s \in \mathcal{S}$ to a vertex j was larger than 1.2 times the Euclidean distance from s to j for all $s \in \mathcal{S}$, then j was removed from the lattice. This technique which we dub *lattice pruning* is to keep the lattice relatively small, and to remove vertices for which the optimal motion requires a large loop. The value of 1.2 comes from the observation that the optimal motion from the start vertex $s = (0, 0, 0, \kappa_{\max})$ to $j = (r_{\min}, r_{\min}, \pi/2, \kappa_{\max})$ is a quarter circular arc of radius r_{\min} . The ratio of the arc-length of this maneuver to the Euclidean distance from s to j is $\pi/(2\sqrt{2}) \approx 1.11$. Thus using a cutoff value of 1.2 admits a sharp left and right quarter turn but is still relatively small.

2) *Adding Reverse Motion*: The motion primitives returned by the MILP in (6) are motions between a starting vertex $s \in \mathcal{S}$, and a lattice vertex $j \in L - \mathcal{S}$. As such, they are for forward motion only. To add reverse motion primitives to the control set E_s for each $s \in \mathcal{S}$, we applied the

forward primitives to \mathcal{S} in reverse. We then rounded the final configurations of these primitives to the closest lattice vertex. For each (x, y) -value of the final configurations, we select a single configuration (x, y, θ, κ) that minimizes arc-length. This is to keep the branching factor of an online search low. Finally, to each $s = (0, 0, \theta, \kappa) \in \mathcal{S}$ we add three primitives: $(0, 0, \theta, \pm\kappa_{\max}), (0, 0, \theta, 0)$ with a reverse motion penalty. These primitives reflect the cars ability to stop and instantaneously change its curvature.

3) *Scenario Results*: We verified our results in four parking lot scenarios (a)-(e). The first four scenarios illustrate our technique in parking lots requiring forward and reverse parking. The results are illustrated in Figure 5. Here, we have compared our approach to Hybrid A* using an identical collision checking algorithm, and using the same heuristic (that proposed in [2]). Though the motions may appear similar, they are actually quite different. This difference is illustrated in Figure 6 which illustrates the heading θ of the vehicle along the motion proposed herein vs that of Hybrid A*. Heading profiles for the other scenarios are not included for brevity, though results are similar. To evaluate the quality of the

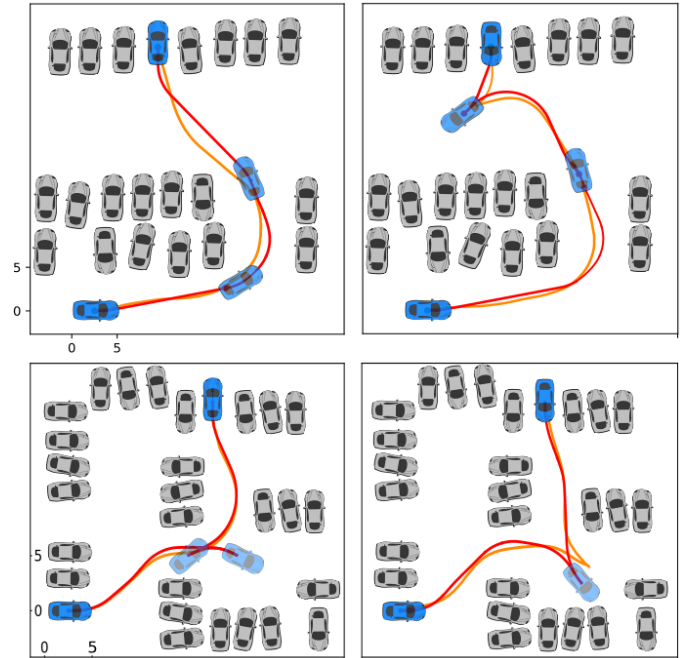


Fig. 5: Scenarios (a) - (d). Red paths from proposed method, yellow from Hybrid A*.

motions predicted, we use three metrics: the integral of the square jerk (IS Jerk), final arc-length, and runtime. These three metrics are expressed as ratios of the value obtained using the methods of [2] to those of the proposed. The results are summarized in Table I. The major difference between the two approaches can be seen in the IS Jerk Reduction. That is, the ratio of the IS Jerk using the methods of [2] to those of the proposed. This is due to the fact that the motion primitives we employ are each G^3 curves with curvature rates bounded by what is known to be comfortable. Thus each motion used during the online search is designed to be optimal. observe that the value of IS Jerk obtained using our approach is up to 16 times less than that of [33]. In fact, using a Hybrid A*

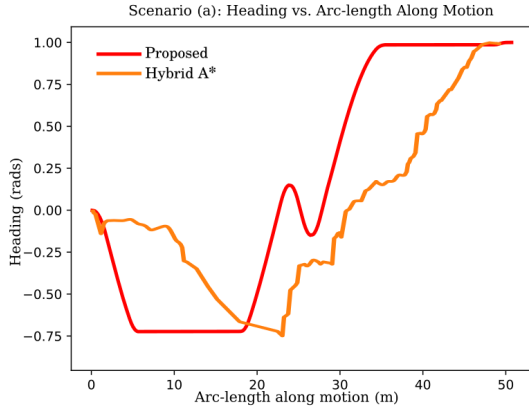


Fig. 6: Heading along Motion for Scenario (a). Orange: Hybrid A* motion, Blue: proposed.

approach may result in motions with infeasibly large curvature rates resulting in larger tracking errors and increased danger to pedestrians.

Despite the bounds on curvature rate, the final arc-lengths of curves computed using our approach are comparable to those of Hybrid A*. Observe that despite the fact that Dubins' paths (which are employed by Hybrid A*) take on average two orders of magnitude less time to compute than G^3 curves, the runtime performance of our method often exceeds that of Hybrid A*. In fact, our proposed method takes, on average 6.9 times less time to return a path, exceeding the runtime speedup of the method proposed in [22]. Moreover, the methods in [22] do not account for reverse motion, and also assume that a set of way-points between start and goal configurations is known.

The only scenario in which Hybrid A* produces a motion in less time than the proposed method is Scenario (c) in which Hybrid A* produced a path with no reverse motion (which accounts for the speedup). However, in order to produce this motion, the curvature of the motion must change instantaneously multiple times resulting in an IS Jerk that is 16.3 times higher than the proposed method.

The increase in runtime performance of the proposed method is due to longer primitives we employ. It has been observed that Hybrid A* often takes several iterations to obtain a motion of comparable length to one of our primitives. This results in a much larger open set during each iteration of A*.

The final scenario we investigated is a parallel parking scenario (scenario (e)) which is illustrated in Figure 7. Though the motion computed with Hybrid A* may appear simpler, it requires a curvature rate that is 16.7 times larger than what is considered comfortable. It should also be noted that several other parallel parking scenarios in which the clearance between obstacles was decreased. While the proposed method returned a path in each of these scenarios, Hybrid A* failed to produce a path in the allotted time.

A final example of a complex parking lot navigation scenario can be found in Figure 1 was generated using the same motion primitives used in this section. This maneuver involves first traversing a parking lot, then parallel parking. Green and blue paths illustrate the two trees rooted at start and goal during the PrAC algorithm. The final motion appears in red.

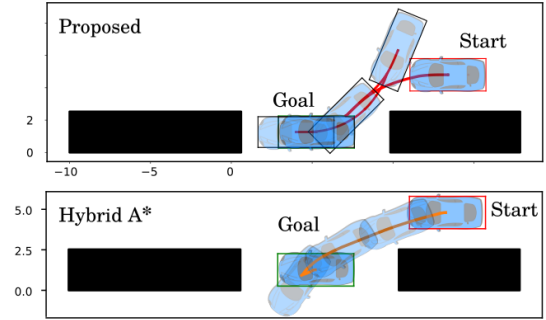


Fig. 7: Scenario (e).

Scenario	IS Jerk Reduction	Length Reduction	Runtime Speedup
(a)	7.7	0.99	5.26
(b)	9.91	1.01	18.40
(c)	10.14	0.96	0.61
(d)	16.32	2.21	7.30
(e)	16.71	0.63	3.00

TABLE I: Scenario Results

C. Speed Lattice

In this experiment, we generate a full trajectory (including both path and speed profile) for use in highway driving using our approach. In this section, we use only forward motion as reverse motion on a highway is unlikely.

In addition to developing G^3 paths, our work in [32] also details a method with which a trajectory with configurations $(x, y, \theta, \kappa, \sigma, \rho, v, a, \beta)$ may be computed. Here, v, a, β represent velocity and longitudinal acceleration, and longitudinal jerk respectively. The approach is to compute bang-bang profiles of ρ and β that result in a trajectory that minimizes a user-specified cost function. This cost function is a weighted sum of undesirable trajectory features including the integral of the square (IS) acceleration, IS jerk, IS curvature, and final arc-length. The key feature of this approach is that both path (controlled by ρ) and velocity profile (controlled by β) are optimized simultaneously, thus keeping path planning in-loop during the optimization. This differs from the common approach which fits a velocity profile over a planned path [22], [3]. It also assumes continuously differentiable velocity as opposed to a more common piece-wise linear velocity [3] in which moments of infinite jerk occur. As in the previous set of examples, computing trajectories via the methods outlined in [32] require orders of magnitude more time than simple Dubins' paths.

However, pre-computing a set of motion primitives where each motion is itself computed using the methods of [32] ensures that every motion used in PrAC is optimal for the user. Moreover, because we include velocity in our configurations – and therefore in our primitives – we do not need to compute a velocity profile.

1) *Lattice Setup & Pruning*: Motion primitives were generated (6) for a 24×32 grid. Dynamic bounds for comfort were kept at (9). The x component of the lattice vertices were sampled every $r_{\min}/6$ meters while the y components were sampled every $r_{\min}/12$. Headings were sampled every $\pi/16$ radians (32 samples). We also assumed values of $\kappa = \sigma =$

$\alpha = 0$ on lattice vertices. To account for off-lattice start-goal pairs, we use a higher-fidelity lattice with 128 headings, and 10 headings between $-\kappa_{\max}, \kappa_{\max}$. Finally, five evenly spaced velocities were sampled between 15 and 20 km/hr. A value of $n = 0$ was used in the smoothing Algorithm 1.

2) *Scenario Results*: The highway scenario was chosen to closely resemble the roadway driving scenario in [22]. The results of this scenario can be found in Figure 8, while performance analysis is summarized in Table II. The metrics used to measure performance are the arc-length of the proposed motion, the smoothness cost of the motion, the maximum curvature obtained over the motion, and a runtime speedup normalized to Hybrid A* (HA*). The final column of the Table indicates whether a velocity profile was included during the motion computation. In Table II, two values of smoothness cost are given in the form of a tuple (Smoothness₁, Smoothness₂). The first value of the tuple refers to the definition of smoothness from [2]: sampling N configurations along a motion, we let \mathbf{x}_i denote vector of x, y -components of the i^{th} configuration. Letting $\Delta\mathbf{x}_i = \mathbf{x}_i - \mathbf{x}_{i-1}$, the first metric of smoothness is given by:

$$\text{Smoothness}_1 = \sum_{i=1}^{N-1} |\Delta\mathbf{x}_{i+1} - \Delta\mathbf{x}_i|^2.$$

The second value of the tuple refers to the definition of smoothness used in [22]. Here, smoothness is given by

$$\text{Smoothness}_2 = \int_0^{s_f} \kappa(s)^2 ds,$$

which is the integral of the squared curvature along the motion to final arc-length s_f . The first two methods appearing in the Table are computed directly from the motions in Figure 8, while the second two come from [22] for an almost identical experiment. Here, CG refers to the method proposed in [22], while HA2* refers to the implementation of Hybrid A* as it appears in [22].

The authors of [22] report an average runtime speedup of 4.5 times as compared to Hybrid A* for the path planning phase (without speed profile). On average, PrAC computed a full motion, including a speed profile 4.7 times faster than the time required for Hybrid A* to compute a path. Furthermore, the use of PrAC with G^3 motion primitives significantly reduced the smoothness cost in both of its possible definitions.

Method	Length (m)	Smoothness Cost	Max Curvature (m^{-1})	Runtime Speedup	Velocity
HA*	65.0	(1.35, 0.77)	0.198	1	No
Proposed	64.6	(0.17, 0.28)	0.158	4.7	Yes
CG	65.8	(-, 0.44)	0.189	4.5	No
HA2*	65.6	(-, 0.88)	0.196	1	No

TABLE II: Road navigation results: HA* and proposed shown above. CG and HA2* from [22] Table 3 for similar motion planning problem.

V. DISCUSSION

The results of the previous section illustrate the effectiveness of the proposed technique. Indeed, feasible, smooth motions

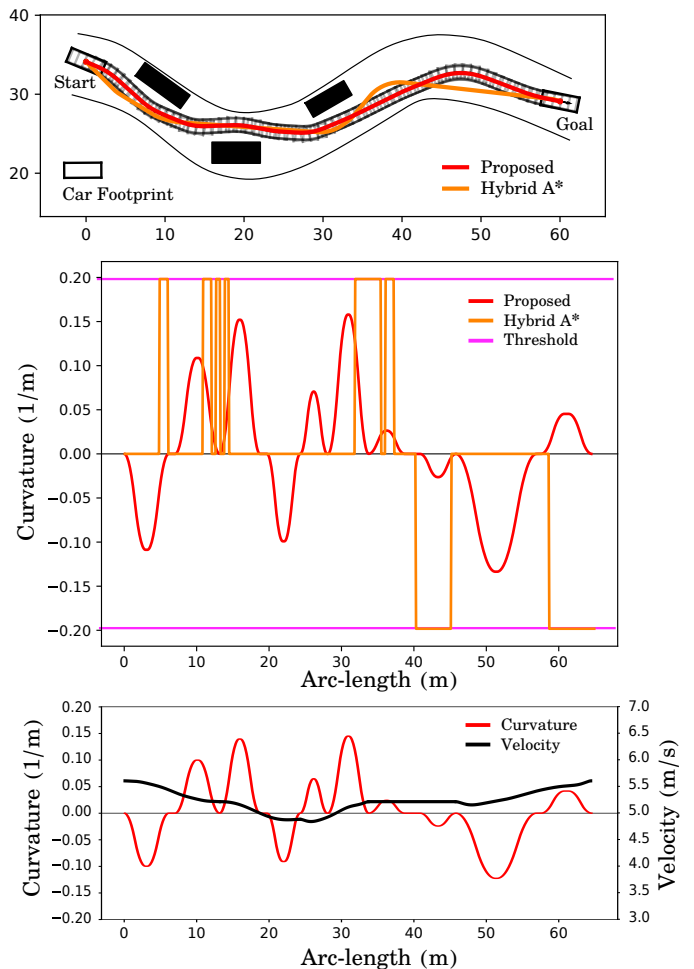


Fig. 8: Result of highway maneuver with several obstacles.

were computed between start and goal locations in both parking lot and highway settings. By adding reverse motion primitives, complex problems like navigating an obstacle-rich parking lot, or parallel parking were solved. Moreover, if the motion primitives already include velocity as a state, then a velocity profile may be easily computed.

However, the methods proposed here would theoretically do less well in situations requiring frequent re-planning. In these situations, the configuration of the vehicle lies predominantly in the higher-fidelity lattice where a larger number of primitives cause an increase in the branching factor.

REFERENCES

- [1] R. Geraerts and M. H. Overmars, “Creating high-quality paths for motion planning,” *The international journal of robotics research*, vol. 26, no. 8, pp. 845–863, 2007.
- [2] D. Dolgov, S. Thrun, M. Montemerlo, and J. Diebel, “Practical search techniques in path planning for autonomous driving,” *Ann Arbor*, vol. 1001, no. 48105, pp. 18–80, 2008.
- [3] Z. Zhu, E. Schmerling, and M. Pavone, “A convex optimization approach to smooth trajectories for motion planning with car-like robots,” in *2015 54th IEEE conference on decision and control (CDC)*. IEEE, 2015, pp. 835–842.
- [4] M. Pivtoraiko and A. Kelly, “Generating near minimal spanning control sets for constrained motion planning in discrete state spaces,” in *2005 IEEE/RSJ International Conference on Intelligent Robots and Systems*. IEEE, 2005, pp. 3231–3237.

- [5] M. Pivtoraiko, R. A. Knepper, and A. Kelly, "Differentially constrained mobile robot motion planning in state lattices," *Journal of Field Robotics*, vol. 26, no. 3, pp. 308–333, 2009.
- [6] L. Janson, B. Ichter, and M. Pavone, "Deterministic sampling-based motion planning: Optimality, complexity, and performance," *The International Journal of Robotics Research*, vol. 37, no. 1, pp. 46–61, 2018.
- [7] A. Botros and S. L. Smith, "Computing a minimal set of t-spanning motion primitives for lattice planners," *arXiv preprint arXiv:1903.10483*, 2019.
- [8] M. Pivtoraiko and A. Kelly, "Kinodynamic motion planning with state lattice motion primitives," in *2011 IEEE/RSJ International Conference on Intelligent Robots and Systems*. IEEE, 2011, pp. 2172–2179.
- [9] K. Yang and S. Sukkarieh, "An analytical continuous-curvature path-smoothing algorithm," *IEEE Transactions on Robotics*, vol. 26, no. 3, pp. 561–568, 2010.
- [10] C. Sprunk, "Planning motion trajectories for mobile robots using splines." Student project, University of Freiburg, Germany, 2008.
- [11] C. G. L. Bianco and A. Piazzì, "Optimal trajectory planning with quintic g/sup 2/-splines," in *IEEE Intelligent Vehicles Symposium (IV)*, 2000, pp. 620–625.
- [12] L. E. Kavradi, P. Svestka, J. . Latombe, and M. H. Overmars, "Probabilistic roadmaps for path planning in high-dimensional configuration spaces," *IEEE Transactions on Robotics and Automation*, vol. 12, no. 4, pp. 566–580, 1996.
- [13] S. M. LaValle, *Planning algorithms*. Cambridge university press, 2006.
- [14] S. Karaman and E. Frazzoli, "Sampling-based algorithms for optimal motion planning," *The International Journal of Robotics Research*, vol. 30, no. 7, pp. 846–894, 2011.
- [15] E. Schmerling, L. Janson, and M. Pavone, "Optimal sampling-based motion planning under differential constraints: the driftless case," in *2015 IEEE International Conference on Robotics and Automation (ICRA)*. IEEE, 2015, pp. 2368–2375.
- [16] L. Janson, E. Schmerling, A. Clark, and M. Pavone, "Fast marching tree: A fast marching sampling-based method for optimal motion planning in many dimensions," *The International journal of robotics research*, vol. 34, no. 7, pp. 883–921, 2015.
- [17] M. Ruffli and R. Siegwart, "On the design of deformable input/state-lattice graphs," in *2010 IEEE International Conference on Robotics and Automation*. IEEE, 2010, pp. 3071–3077.
- [18] M. McNaughton, C. Urmson, J. M. Dolan, and J.-W. Lee, "Motion planning for autonomous driving with a conformal spatiotemporal lattice," in *IEEE International Conference on Robotics and Automation*, 2011, pp. 4889–4895.
- [19] M. Dharmadhikari, T. Dang, L. Solanka, J. Loje, H. Nguyen, N. Khedekar, and K. Alexis, "Motion primitives-based path planning for fast and agile exploration using aerial robots," in *2020 IEEE International Conference on Robotics and Automation (ICRA)*, 2020, pp. 179–185.
- [20] D. Dolgov, S. Thrun, M. Montemerlo, and J. Diebel, "Path planning for autonomous vehicles in unknown semi-structured environments," *The international journal of robotics research*, vol. 29, no. 5, pp. 485–501, 2010.
- [21] J. Levinson, J. Askeland, J. Becker, J. Dolson, D. Held, S. Kammel, J. Z. Kolter, D. Langer, O. Pink, V. Pratt *et al.*, "Towards fully autonomous driving: Systems and algorithms," in *2011 IEEE Intelligent Vehicles Symposium (IV)*. IEEE, 2011, pp. 163–168.
- [22] Y. Zhang, H. Chen, S. L. Waslander, J. Gong, G. Xiong, T. Yang, and K. Liu, "Hybrid trajectory planning for autonomous driving in highly constrained environments," *IEEE Access*, vol. 6, pp. 32 800–32 819, 2018.
- [23] A. Paraschos, C. Daniel, J. R. Peters, and G. Neumann, "Probabilistic movement primitives," *Advances in neural information processing systems*, vol. 26, pp. 2616–2624, 2013.
- [24] L. Jarin-Lipschitz, J. Paulos, R. Bjorkman, and V. Kumar, "Dispersion-minimizing motion primitives for search-based motion planning," *arXiv preprint arXiv:2103.14603*, 2021.
- [25] L. Palmieri, L. Bruns, M. Meurer, and K. O. Arras, "Dispertio: Optimal sampling for safe deterministic motion planning," *IEEE Robotics and Automation Letters*, vol. 5, no. 2, pp. 362–368, 2019.
- [26] D. Peleg and A. A. Schäffer, "Graph spanners," *Journal of graph theory*, vol. 13, no. 1, pp. 99–116, 1989.
- [27] P. Carmi and L. Chaitman-Yerushalmi, "Minimum weight euclidean t-spanner is NP-hard," *Journal of Discrete Algorithms*, vol. 22, pp. 30–42, 2013.
- [28] A. Botros, N. Wilde, and S. L. Smith, "Learning control sets for lattice planners from user preferences," in *The 14th International Workshop on the Algorithmic Foundations of Robotics (WAFR)*, volume: To appear, 2020.
- [29] B. Korte, J. Vygen, B. Korte, and J. Vygen, *Combinatorial optimization*, 6th ed. Springer, 2018.
- [30] J. Desrosiers, Y. Dumas, M. M. Solomon, and F. Soumis, "Time constrained routing and scheduling," *Handbooks in operations research and management science*, vol. 8, pp. 35–139, 1995.
- [31] J. J. Kuffner and S. M. LaValle, "Rrt-connect: An efficient approach to single-query path planning," in *Proceedings 2000 ICRA. Millennium Conference. IEEE International Conference on Robotics and Automation. Symposia Proceedings (Cat. No. 00CH37065)*, vol. 2. IEEE, 2000, pp. 995–1001.
- [32] A. Botros and S. L. Smith, "Tunable trajectory planner using g3 curves," *arXiv 2106.03836*, 2021.
- [33] H. Banzhaf, N. Berinpanathan, D. Nienhüser, and J. M. Zöllner, "From G2 to G3 continuity: Continuous curvature rate steering functions for sampling-based nonholonomic motion planning," in *2018 IEEE Intelligent Vehicles Symposium (IV)*. IEEE, 2018, pp. 326–333.